The Bifurcation Set for the 1:4 Resonance Problem

Bernd Krauskopf

CONTENTS

We study the bifurcation set in (b, φ, α)-space of the equation $\dot{z} = e^{i\alpha} z + e^{i\varphi} z\,|z|^2 + b\bar{z}^3$. This $\mathbb{Z}_4$-equivariant planar vector field is equivalent to the model equation that has been considered in the study of the 1:4 resonance problem.

We present a three-dimensional model of the bifurcation set that describes the known properties of the system in a condensed way, and, under certain assumptions for which there is strong numerical evidence, is topologically correct and complete. In this model, the bifurcation set consists of surfaces of codimension-one bifurcations that divide (b, φ, α)-space into fifteen regions of generic phase portraits. The model also offers further insight into the question of versality of the system. All bifurcation phenomena seem to unfold generically for $\varphi \neq \pi/2,\ 3\pi/2$.

1. INTRODUCTION

The problem of 1:q resonance of a closed orbit of a vector field in $\mathbb{R}^3$ has been solved except for the case $q = 4$ [Arnol'd 1977; 1988; Arnol'd et al. 1994; Carr 1981; Takens 1974]. This paper is concerned with the open case of 1:4 resonance. The Poincaré map on a section transversal to the closed orbit can be approximated by the time-one map of a $\mathbb{Z}_4$-equivariant planar vector field composed with the rotation by a quarter-turn. From now on we stay in the context of planar vector fields. A $\mathbb{Z}_4$-equivariant planar vector field can be brought to the normal form

$$\dot{z} = \varepsilon z + Az\,|z|^2 + B\bar{z}^3 + O(|z|^5),$$

where $\varepsilon, A, B \in \mathbb{C}$. The idea of solving the problem is to consider the *principal part*

$$\dot{z} = \varepsilon z + Az\,|z|^2 + B\bar{z}^3 \tag{1.1}$$

and answer the following interdependent questions:

1058-6458/96 $0.50 per page

1. What kinds of bifurcation phenomena can occur in the principal part, and for what values of the parameters do they occur?
2. Is the principal part a versal unfolding?

(Roughly speaking, the second question asks if the family (1.1) is big enough that all bifurcation phenomena in it are generic.)

The idea of the study is to address the first question in order to show that all occurring bifurcation phenomena are robust under perturbations caused by the higher-order terms, thus solving also the second question. This has led to solving the problem of 1:q resonance for $q \neq 4$. In the 1:4 case it is conjectured that (1.1) is indeed a versal unfolding [Arnol'd 1977; 1988; Arnol'd et al. 1994; Takens 1974].

The classic approach of the analysis of (1.1) is as follows [Arnol'd 1988; Arnol'd et al. 1994, pp. 57–60; Berezovskaia and Khibnik 1980; Chow 1994; Krauskopf 1994]. By scaling, the number of real parameters in (1.1) can be reduced to three, as explained in Section 2. We use the reduction

$$\dot{z} = e^{i\alpha} z + e^{i\varphi} z\, |z|^2 + b\bar{z}^3, \tag{1.2}$$

which assumes $A \neq 0$. Here $b \in \mathbb{R}^+$, $\varphi \in (-\pi, \pi]$ and $\alpha \in (-\pi, \pi]$. Due to reflectional symmetries, it is sufficient to consider the case $\varphi \in [\pi, 3\pi/2]$.

For fixed (b, φ) one considers the dynamics of (1.2) as $\varepsilon = e^{i\alpha}$ varies along the unit circle. The *bifurcation sequence* for this (b, φ) is the sequence of topologically different phase portraits as α varies. We call two bifurcation sequences *equivalent* if the same types of bifurcations occur in the same order and the respective phase plane pictures are topologically equivalent. Thus the unfolding in $\varepsilon = e^{i\alpha}$ for a given (b, φ) is determined by its bifurcation sequence.

By dividing the (b, φ)-plane into regions of equivalent bifurcation sequences, we get a catalogue of bifurcation sequences, or a parametrization of the unfoldings in $\varepsilon = e^{i\alpha}$ of the singularity at $\varepsilon = 0$. Crossing from one region to another changes the equivalence type of the bifurcation sequences.

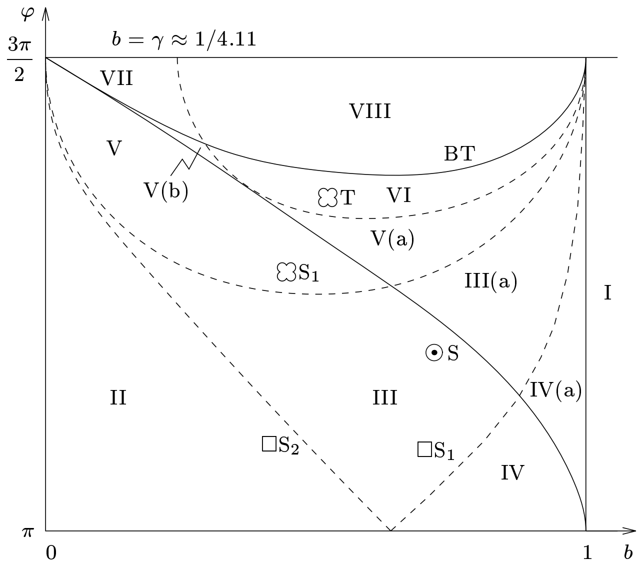

FIGURE 1. The third quadrant of the (b, φ)-plane of the compact equation (1.2), showing the regions of different bifurcation sequences (roman numerals). The regions are labeled as in [Krauskopf 1994]; the corresponding bifurcation sequences are also given there, but will be clear from the present discussion. For the curve labels, see Section 2. The solid curves are known analytically; the dashed ones are not, but are adapted from the numerical results in [Berezovskaia and Khibnik 1978; 1980].

The partition of the (b, φ)-plane for this problem is shown in Figure 1.

Equivalence of bifurcation sequences is a fairly difficult notion to study. Instead of dividing the (b, φ)-plane into regions of equivalent bifurcation sequences, a more natural approach, traditionally used in bifurcation theory, is to divide the full parameter space, or (b, φ, α)-space, into regions of topologically equivalent phase portraits, and try to study the boundaries between these regions. This is the approach taken in this paper.

Thus our goal is to analyze the bifurcation set in (b, φ, α)-space for the system (1.2). All the interesting behavior for this system occurs in a compact subset of parameter space, namely $b \in [0, 1]$, as shown in Figure 1. We call (1.2) the *compact equation*, and we call the region $\alpha \in (-\pi, \pi]$, $\varphi \in [\pi, 3\pi/2]$, $b \in [0, 1]$ the *cube of interest*.

The bifurcation set consists of surfaces of bifurcations of codimension one, typically meeting in curves of codimension-two bifurcations. As we shall see, it divides (b, φ, α)-space into fifteen regions of generic phase portraits. Since the region of interest is compact, it is relatively easy to illustrate the bifurcation set: this will be done in Figures 9 and 10. This three-dimensional set, plus the fifteen types of generic phase portraits, account for the known properties of the compact equation (1.2) in a condensed way in the spirit of bifurcation theory.

All the information about the (b, φ)-plane and the bifurcation sequences can be extracted from the bifurcation set. In order to construct a bifurcation sequence for a given (b, φ), all one has to do is collect the equivalence types of phase portraits that occur as α varies, say, from $-\pi$ to π, much as one drills into glacial ice to learn about the climate of previous ages. The transition from one generic phase portrait to the next goes via a generic codimension-one bifurcation if the drilling only intersects codimension-one parts of the bifurcation set (surfaces), and then only transversely. This happens when (b, φ) is not on one of the boundary curves of Figure 1. In other words, the curves shown in Figure 1 are projections in the (b, φ)-plane of the locus of higher-codimension bifurcation in (b, φ, α)-space.

Actually, the bifurcation set in (b, φ, α)-space contains *more* information than the division of the (b, φ)-plane combined with the knowledge of the bifurcation sequences. This is because it also shows what happens above the boundary curves in the (b, φ)-plane.

The study of the bifurcation set allows conclusions about the versality of the system. For $\varphi \neq 3\pi/2$, that is, in the interior of the cube of interest, all known bifurcation phenomena seem to unfold generically. In particular, there do not seem to be singularities of codimension higher than two.

More precisely, it is conjectured that (1.2) is a versal unfolding in the regions of the (b, φ)-plane corresponding to the known bifurcation sequences, and that there are no bifurcation sequences other than the known ones.

The first issue that must be addressed in order to verify this conjecture concerns the nature of the surfaces of codimension-one bifurcations. Numerical experiments consisting of phase plane studies with the program package DsTool [Back et al. 1992] and the computation of two-dimensional cross sections of the model with the continuation package Auto [Doedel 1986] suggest that the surfaces do not intersect in curves of codimension-two bifurcations other than the known ones, and do not have folds with respect to α. Assuming this is true (Assumption 3.10), we can give a topologically correct description of the bifurcation set.

The second issue is the nature of the curves of codimension-two bifurcations. Are they generic or are there points of higher codimension on them that give rise to yet unknown surfaces of codimension-one bifurcation? The study of the bifurcation set shows that the curves do not intersect in the interior of the cube of interest. Furthermore, numerical evidence indicates that the curves of codimension-two bifurcations are generic inside the cube. By this we mean that a transversal section of such a curve shows locally, around the point of intersection, the two-dimensional bifurcation diagram that is to be expected for the generic codimension-two bifurcation in question. In short, there do not seem to be points of higher codimension on the curves.

The third issue concerns the nature of the bifurcations for $\varphi = 3\pi/2$, on the boundary of the cube of interest. These bifurcations can give rise to surfaces of codimension-one bifurcations inside the cube. The best example of this is the study of the Hamiltonian cases for $\alpha = \pm\pi/2$ [Neishtadt 1978]. They are of infinite codimension and organize the surfaces of codimension-one bifurcations. The line $b = 1$, $\varphi = 3\pi/2$, $\alpha \in (-\pi, \pi]$ plays a similar role. The study of the bifurcation set shows that the surfaces of codimension-one bifurcations accumulate on this line, and that the singularities for parameter values on this line are of codimension at least two, and of higher codimension for $\alpha = -\pi/2$, 0, $\pi/2$, π. The study of these bifurcations is in progress and will be the topic of a later paper.

This article is organized as follows. Section 2 explains how the family (1.1) is reduced to (1.2) or to the model equation found in the literature, and how the two reductions are related; it also describes the boundary curves in the (b, φ)-plane. Section 3 is devoted to the bifurcation set in (b, φ, α)-space, which consists of *local surfaces* and *nonlocal surfaces*. Local surfaces are those characterized by local bifurcations, namely, Hopf and saddle-node bifurcations. Their parametrizations and intersection curves can be calculated analytically from conditions on equilibria. This is done in Section 3.1 for the case $b < 1$. Nonlocal surfaces are characterized by the relative positions of stable and unstable manifolds, and have no known parametrizations. In Section 3.2 we "model" these surfaces for the case $b < 1$, that is, we study their position relative to one another and to the local surfaces. This leads to the three-dimensional illustrations of the bifurcation set in Figures 9 and 10. Section 3.3 deals with the simple case $b > 1$, giving the bifurcation set for region I. Section 4 returns to the question of genericity of the bifurcations of codimensions one and two, discussed in the preceding paragraphs.

2. BACKGROUND

This section discusses what is known about the (b, φ)-plane of the compact equation (1.2).

In the literature of the 1:4 resonance problem [Arnol'd 1988; Arnol'd et al. 1994; Berezovskaia and Khibnik 1980; Chow 1994; Krauskopf 1994] the reader will find the reduction of (1.1) to the *model equation*

$$\dot{z} = e^{i\alpha} z + Az\,|z|^2 + \bar{z}^3, \tag{2.1}$$

which assumes $B \neq 0$. Due to reflectional symmetries in the phase plane it is sufficient to consider the case $\operatorname{Re} A < 0$, $\operatorname{Im} A < 0$.

The equivalent of the (b, φ)-plane of the compact (1.2) is the A-plane of the model equation (2.1) shown in Figure 2. The two equations are related by

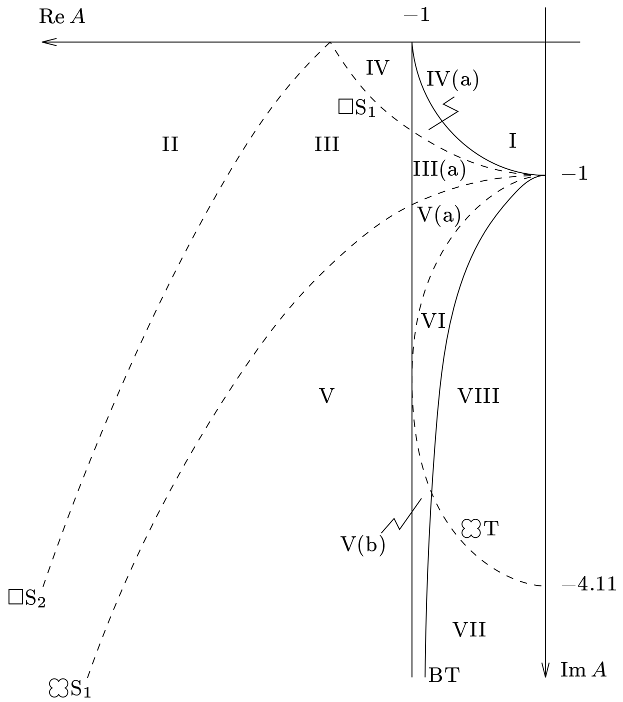

FIGURE 2. The well-known A-plane of the model equation (2.1). Each region corresponds to one equivalence class of bifurcation sequences for the system. The dashed curves were calculated by continuation in [Berezovskaia and Khibnik 1978; 1980]. This is an image of Figure 1 under the transformation (2.2).

$$\operatorname{Re} A = \frac{1}{b}\cos\varphi, \qquad \operatorname{Im} A = \frac{1}{b}\sin\varphi. \tag{2.2}$$

We now give a geometrical explanation of the connection between the two different reductions.

The idea of the reduction of (1.1) is to quotient parameter space by the equivalence relations induced by rescaling space and time. Rescaling z by $\bar{c} \in \mathbb{C}$ shows that the triple (ε, A, B) is equivalent to $(\varepsilon,\ |c|^2 A,\ c^4/|c|^2 B)$.

Next, rescaling time by $r \in \mathbb{R}^+$ gives the equivalences $(\varepsilon, A, B) \sim (r\varepsilon,\ rA,\ rB) \sim (r\varepsilon, A, B)$. This means that the bifurcation curves in the ε-plane are straight lines starting at the origin, and we can replace ε by $e^{i\alpha}$, where $\alpha \in (-\pi, \pi]$. It follows

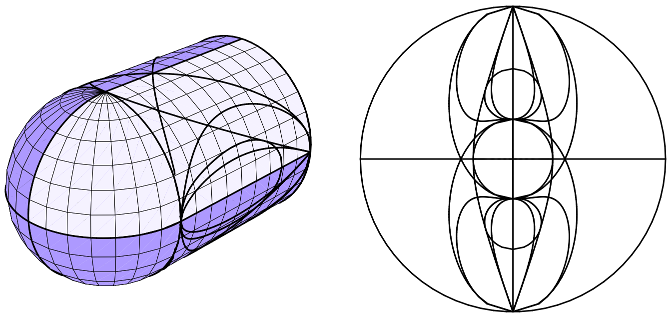

FIGURE 3. Illustrating the compactification. Left: The half-cylinder (b, φ), for $\varphi \in [0, 2\pi]$ and $b \in \mathbb{R}_+$, is compactified by a point $b = \infty$ to give a surface shaped like a goblet. The lightly shaded region is the third quadrant of the (b, φ)-plane, shown in Figure 1. Right: Looking into the goblet shows the compactification of the A-plane by a circle.

that (1.1) can be reduced to the compact equation (1.2), with loss of the case $A = 0$. This missing case corresponds to $b = \infty$, so we could compactify the (b, φ)-plane by adjoining this point (Figure 3, left).

Analogously, (1.1) can be reduced to the model equation (2.1), with loss of the case $B = 0$. We could think of $B = 0$ as corresponding to a circle of points with $A = \infty$ in (2.1), thus compactifying the parameter space into a disk (Figure 3, right).

Finally, we do not wish to distinguish between phase portraits that can be transformed into each other by the transformations $(z, t) \mapsto (\bar{z}, t)$ and $(z, t) \mapsto (\bar{z}, -t)$. This gives the equivalences

$$(\varepsilon, A, B) \sim (\bar{\varepsilon}, \bar{A}, \bar{B}) \sim (-\bar{\varepsilon},\, -\bar{A},\, -\bar{B}),$$

so we can assume $\varphi \in [\pi, 3\pi/2]$ and $\operatorname{Re} A < 0$, $\operatorname{Im} A < 0$ respectively.

As a prerequisite for further considerations we discuss the characterizing properties of the boundary curves in the (b, φ)-plane. This is simply recalling what is known about the A-plane (see references at the beginning of this section). For ease of reference, Table 1 summarizes the notation, and Figures 4 and 5 show the fifteen generic phase portraits that can occur in (1.2). The sketches in the middle of these figures are cross sections of the bifurcation set that will be explained in Section 3.

Curve	Characterizing property	
$\odot$S	Hopf bifurcation at 0 coincides with second saddle-node bifurcation	L
BT	Bogdanov–Takens bifurcation	L
☘T	Clover connection with zero trace	NL
☘S_1	Clover connection coincides with first saddle-node bifurcation	NL
$\square S_1$	Square connection coincides with first saddle-node bifurcation	NL
$\square S_2$	Square connection coincides with second saddle-node bifurcation	NL

TABLE 1. Symbols for curves of codimension-two bifurcations. The notation reflects the characterization of each curve as the intersection of two surfaces (see Table 2). Local and nonlocal curves (see text) are marked L and NL. We use the same symbol for a curve in (b, φ, α)-space and for its projection in the (b, φ)-plane.

The solid curves in Figure 1 have analytic parametrizations, being characterized by local conditions. We will call them *local curves*. They are:

- The line $b = 1$. For $b > 1$ there are four saddle points for any value of α (region I in Figure 1); see phase portraits 11–15 in Figure 5. For $b < 1$ there is an interval of α-values where there exist eight secondary equilibria (that is, equilibria other than the origin): see phase portraits 3, 5–8 in Figure 4. Exactly four of these equilibria are saddle points; the others may be sources or sinks, and we refer to them as nodes.
- The curve $\odot$S, with equation $\varphi = \pi + \arccos b$, where for some α a saddle-node bifurcation of secondary equilibria coincides with a Hopf bifurcation at the origin. Thus, on one side of this curve we have a sequence of phase portraits looking like $9 \to 10 \to 1$ in Figure 4 (for increasing α), and on the other side like $9 \to 11 \to 1$.
- The curve BT where for some α the system has four Bogdanov–Takens points, corresponding to a saddle-node bifurcation with trace zero (thus both eigenvalues are zero at the bifurcating equilibrium). On one side we have a simple

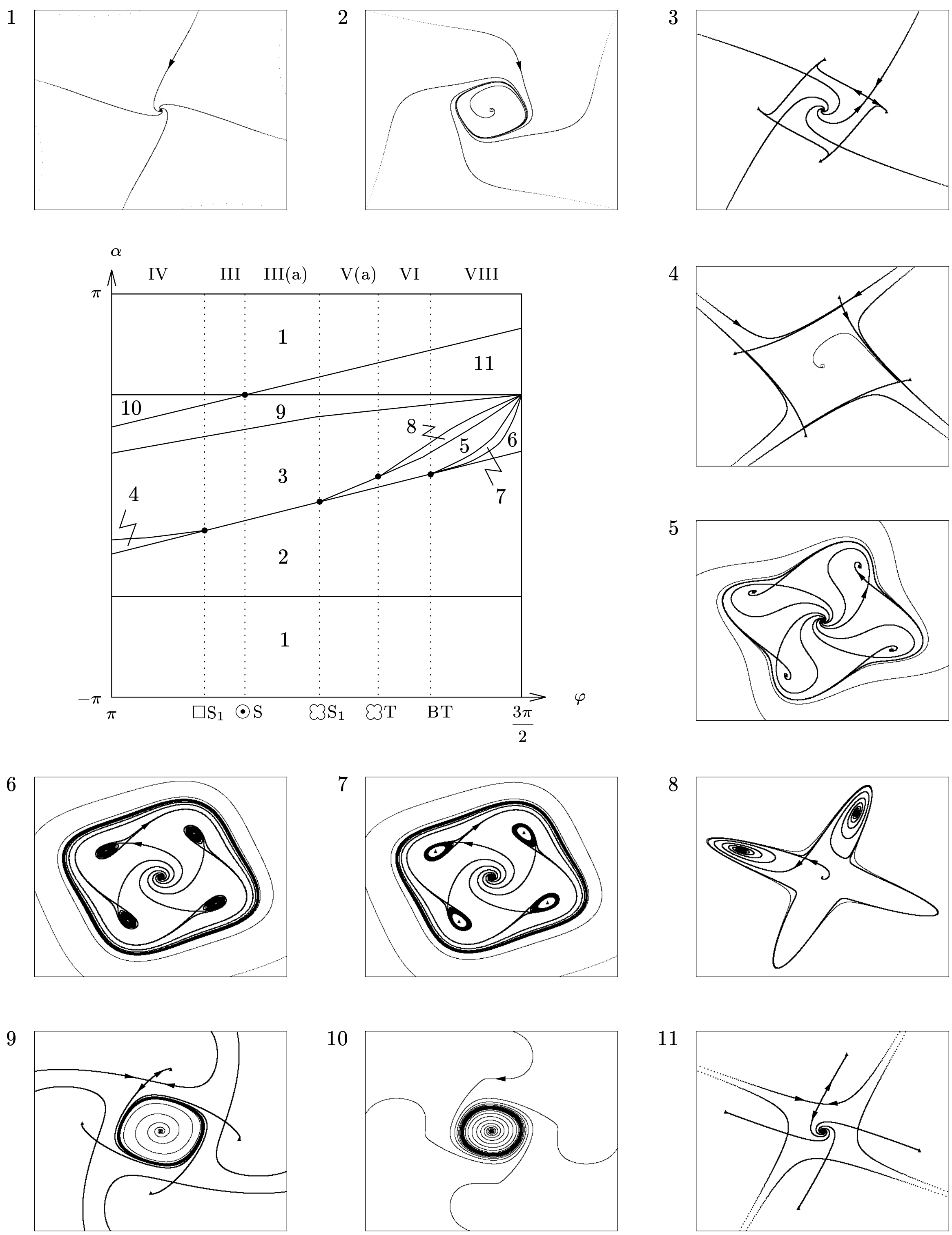

FIGURE 4. All eleven open regions in (b, φ, α)-space and the corresponding different types of generic phase portraits for $b \in (0, 1)$. In panel 8, there are two limit cycles close together, the inner one being where one leaf of the saddles' stable manifold accumulates. The sketch in the middle is a cross section of the bifurcation set for $b \approx 0.8$ (Section 3; see also Figure 14).

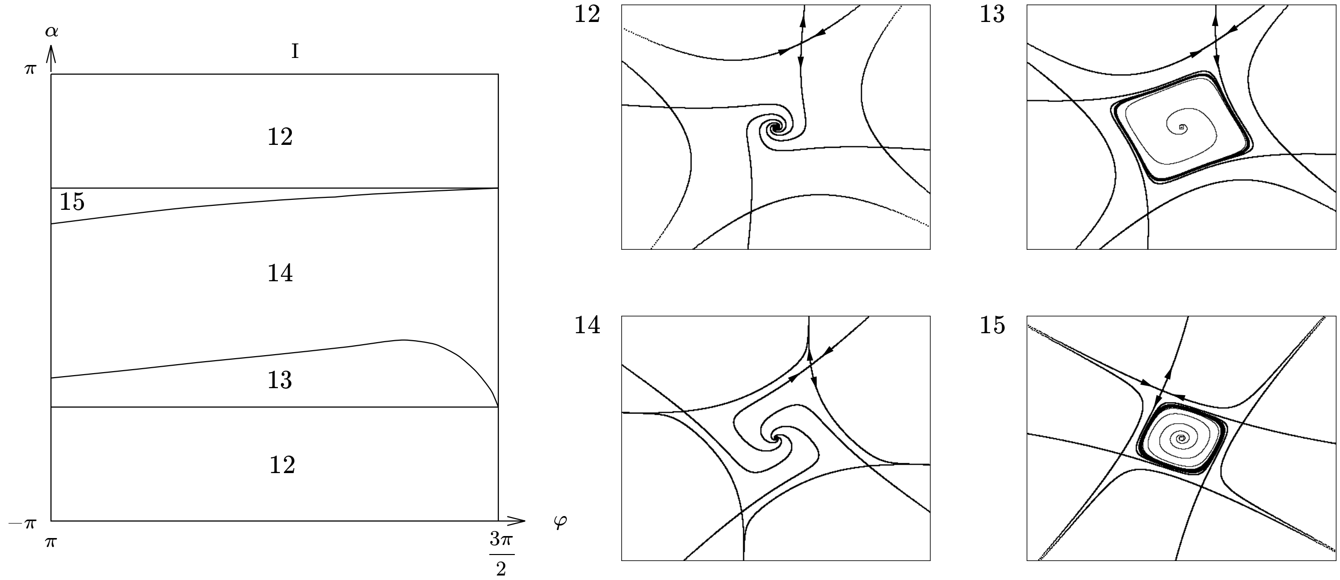

FIGURE 5. The four open regions in (b, φ, α)-space and the corresponding different types of generic phase portraits for $b > 1$. On the left is the sketch of a cross section of the bifurcation set for $b > 1$ (Section 3.3; see also Figure 15).

saddle-node bifurcation, such as $2 \to 5$ in Figure 4, while on the other side we have the sequence $2 \to 6 \to 7 \to 5$, going through a homoclinic connection and a Hopf bifurcation at the secondary equilibria.

The dashed curves in Figure 1 have no known analytic parametrizations: they can only be determined by numerical methods. We refer to them as *nonlocal curves* since they are characterized by the relative positions of the stable and unstable manifolds of saddles depicted in Figure 6. Due to their shapes we call the heteroclinic connection in the second panel of Figure 6 a *square connection* and the one in the fourth panel a *clover connection.* For $b \in (0, 1)$ there are two saddle-node bifurcations, labeled *first* and *second* in order of increasing $\alpha \in (-\pi, \pi]$. Here is a list of the dashed curves in Figure 1:

- On $\square \mathrm{S}_1$ there is a square connection at the moment of the first saddle-node bifurcation. Thus on one side we might have the sequence of phase portraits $2 \to 3$, on the other $2 \to 4 \to 3$.
- On $\square \mathrm{S}_2$ there is a square connection at the moment of the second saddle-node bifurcation. For example, $3 \to 10$ versus $3 \to 9 \to 10$.
- On ⌘S_1 there is a clover connection at the moment of the first saddle-node bifurcation. For example, $2 \to 3$ versus $2 \to 5 \to 3$.

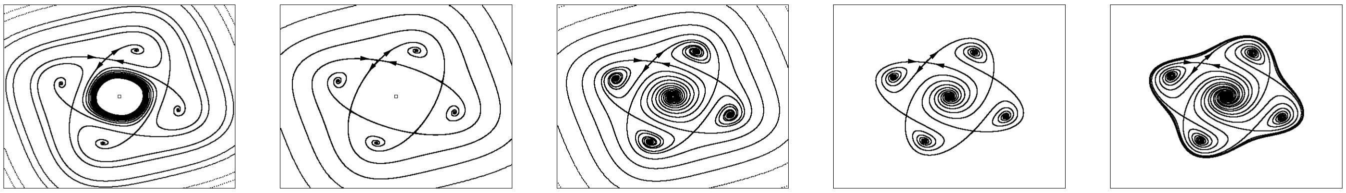

FIGURE 6. Possible relative positions of the stable and unstable manifolds of the saddles: the extreme and middle situations are generic, while the second and fourth are saddle connections of codimension one, called a *square connection* and a *clover connection*, respectively.

- On ☘T there is a clover connection at the moment when the trace at the saddle points is zero. This leads to the birth of two limit cycles. For example, $5 \to 3$ versus $5 \to 8 \to 3$.

We did not recalculate these curves in order to plot Figure 1, but used transformation (2.2) together with the data and asymptotic expressions given in [Berezovskaia and Khibnik 1978; 1980].

3. THE BIFURCATION SET

This section's aim is to give a complete description of the bifurcation set of the compact equation (1.2). We first look at the situation inside the cube of interest $b \in [0,1]$, $\varphi \in [\pi, 3\pi/2]$, $\alpha \in [-\pi,\pi]$. Section 3.1 gives the parametrizations of the local surfaces, and in Section 3.2 we model the nonlocal surfaces. Section 3.3 deals with the bifurcation set for $b > 1$, that is, outside the cube.

3.1. The Local Surfaces for $b \in [0, 1]$

We derive the parametrizations for all local surfaces of codimension-one bifurcations and for their curves of intersection. This constitutes the framework for the modeling of the surfaces of nonlocal codimension-one bifurcations in the next section.

Surface	Characterizing property	
$\odot$	Hopf bifurcation at the origin	L
S_1	First saddle-node bifurcation	L
S_2	Second saddle-node bifurcation	L
T_-	Trace is zero at the saddles	L
T_+	Trace is zero at the nodes (Hopf bifurcation of secondary equilibria)	L
$\square$	Square connection (Figure 6)	NL
☘	Clover connection (Figure 6)	NL
♀	Homoclinic loops of secondary equilibria	NL
$\circledcirc$	Saddle-node bifurcation of limit cycles	NL

TABLE 2. Symbols for surfaces of codimension-one bifurcations. The last column indicates whether the surface is local or not.

Theorem 3.1. *The following local surfaces are in the bifurcation set* (see Figure 9, top left, and Figure 11).

(a) *Two planes of Hopf bifurcations of the origin, denoted* $\odot$ *and having equation* $\alpha = \pm\pi/2$. *The limit cycles occur for* $\alpha \in (-\pi/2, \pi/2)$ *and are attracting.*

(b) *The plane* $b = 1$, *characterized as follows. For* $b > 1$ *there are four secondary equilibria, which are saddle points, for any* α. *For* $b < 1$ *there is an interval of* α*-values where there exist eight secondary equilibria.*

(c) *For* $0 < b < 1$ *there are two surfaces of saddle-node bifurcations* $\alpha = \varphi - \pi \mp \arcsin b$, *denoted* S_1 *and* S_2 *in order of increasing* α. *For*

$$\alpha \in (\varphi - \pi - \arcsin b,\ \varphi - \pi + \arcsin b)$$

there are eight secondary equilibria: the four closest to the origin are saddles, and the other four are nodes.

(d) *The trace-zero surface of the nodes, where the sum of the eigenvalues at a node is zero. This surface is denoted* T_+ *and has equation*

$$\tan\alpha = \frac{1}{2\cos\varphi}\left(\sin\varphi - \sqrt{b^2 - \cos^2\varphi}\right)$$

for

$$\pi + \arccos\sqrt{\frac{b^2(1-b^2)}{3b^2+1}} < \varphi < \frac{3\pi}{2}.$$

It is also characterized as the surface of Hopf bifurcations of the secondary equilibria. The bifurcating limit cycles are repelling. This surface contains the line segment $b = 1$, $\varphi = 3\pi/2$, $\alpha \in [0, \pi/2]$.

Proof. We will work sometimes with the complex form of (1.2),

$$\dot z = f(z,\bar z) = e^{i\alpha} z + e^{i\varphi} z^2 \bar z + b\bar z^3,$$

with derivatives

$$f_z = \tfrac{1}{2}(f_x - i f_y), \qquad f_{\bar z} = \tfrac{1}{2}(f_x + i f_y),$$

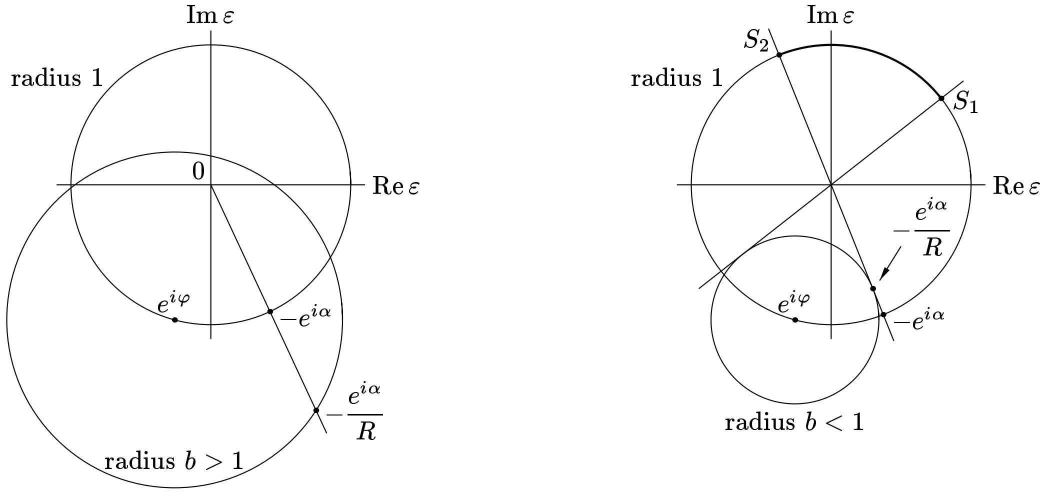

FIGURE 7. Consider how the circle with center $e^{i\varphi}$ and radius b, representing the right-hand side of (3.1), and the ray from the origin through $-e^{i\alpha}$, representing the left-hand side, intersect. Left: for $b > 1$ there is exactly one intersection, and thus four secondary equilibria, for any α. Right: for $0 < b < 1$ there is an interval of values of α for which there are two intersections, giving eight secondary equilibria. For values of α at both ends of this interval, there is one intersection (tangency); these values correspond to the saddle-node bifurcations S_1 and S_2.

and sometimes with the real form,

$$\begin{pmatrix} \dot{x} \\ \dot{y} \end{pmatrix} = \begin{pmatrix} g(x,y) \\ h(x,y) \end{pmatrix},$$

where

$$\begin{aligned} g(x,y) &= x\cos\alpha - y\sin\alpha + b(x^3 - 3xy^2) \\ &\quad + \cos\varphi(x^3 + xy^2) - \sin\varphi(x^2y + y^3), \\ h(x,y) &= y\cos\alpha + x\sin\alpha + b(y^3 - 3x^2y) \\ &\quad + \cos\varphi(x^2y + y^3) + \sin\varphi(x^3 + xy^2). \end{aligned}$$

(a) Since for $\alpha \in (-\pi/2, \pi/2)$ the linear part is unstable at the origin we only need to show that the Hopf bifurcation is supercritical. Using the real notation one gets for the linearization at the Hopf bifurcations of the origin

$$A(\pm\pi/2) = \begin{pmatrix} 0 & \mp 1 \\ \pm 1 & 0 \end{pmatrix}.$$

We now use the stability formula in [Wang 1990]. Here it reduces to

$$K(\pm\pi/2) = (g_{xxx} + h_{xxy}) + (g_{xyy} + h_{yyy}) = 16\cos\varphi < 0$$

for $\varphi \in [\pi, 3\pi/2)$. Consequently the Hopf bifurcations are supercritical.

(b) Let $\sqrt{R}\,e^{i\theta}$ be an equilibrium. Substituting in (1.2) gives

$$-\frac{e^{i\alpha}}{R} = e^{i\varphi} + be^{-4i\theta}. \tag{3.1}$$

Interpreting this equation geometrically (Figure 7), it is easy to see that there are four secondary equilibria for $b > 1$, and either zero, four or eight for $b < 1$. (Compare the circle construction in [Arnol'd 1988].)

(c) Saddle-node bifurcations occur for such values of α that the ray and the circle of Figure 7 are tangent (see the right-hand part of the figure). It is easy to see that these values are $\alpha = \varphi - \pi \mp \arcsin b$. To calculate the equilibria $\sqrt{R}\,e^{i\theta}$, write (3.1) as

$$e^{-4i\theta} = \frac{-e^{i\alpha} - Re^{i\varphi}}{bR}, \tag{3.2}$$

and obtain two equivalent equations for θ:

$$\cos 4\theta = -\frac{\cos\alpha}{bR} - \frac{\cos\varphi}{b}, \quad \sin 4\theta = \frac{\sin\alpha}{bR} + \frac{\sin\varphi}{b}. \tag{3.3}$$

Taking the absolute value of (3.2) and using simple trigonometric equalities gives

$$1+2R\cos(\alpha-\varphi)+(1-b^2)R^2=0, \tag{3.4}$$

or, equivalently,

$$R=\frac{\pm\sqrt{b^2-\sin^2(\alpha-\varphi)}-\cos(\alpha-\varphi)}{1-b^2}. \tag{3.5}$$

The determinant of the system is

$$\begin{aligned}|Df(z,\bar z)| &= f_z\overline{f_z}-f_{\bar z}\overline{f_{\bar z}}\\ &= 1+3\,|z|^4+4\cos(\alpha-\varphi)|z|^2\\ &\qquad -6b\,(\cos\varphi\,\mathrm{Re}\,z^4-\sin\varphi\,\mathrm{Im}\,z^4)\\ &\qquad -9b^2\,|z|^4.\end{aligned}$$

At the secondary equilibria, using (3.3) and later (3.4), this gives after simplification:

$$|Df(\sqrt{R}\,e^{i\theta},\sqrt{R}e^{-i\theta})|=-8(1+\cos(\alpha-\varphi)R).$$

For the equilibria closer to the origin, we have:

$$\begin{aligned}&1+\cos(\alpha-\varphi)R\\ &=1+\cos(\alpha-\varphi)\frac{-\sqrt{b^2-\sin^2(\alpha-\varphi)}-\cos(\alpha-\varphi)}{1-b^2}\\ &=\frac{1-b^2-\cos^2(\alpha-\varphi)-\sqrt{b^2-\sin^2(\alpha-\varphi)}\cos(\alpha-\varphi)}{1-b^2}\\ &=\frac{b^2+\sin^2(\alpha-\varphi)+\sqrt{b^2-\sin^2(\alpha-\varphi)}\sqrt{1-\sin^2(\alpha-\varphi)}}{1-b^2}\\ &>0;\end{aligned}$$

here the first equality comes from (3.5), the third is true because $\cos(\alpha-\varphi)<0$ for

$$\alpha\in(\varphi-\pi-\arcsin b,\ \varphi-\pi+\arcsin b),$$

and the inequality is true because $0<b<1$. This shows the equilibria are saddles.

(d) The trace of the linear part is

$$\mathrm{tr}(Df(z,\bar z))=f_z+\overline{f_z}=2\cos\alpha+4\cos\varphi\,|z|^2. \tag{3.6}$$

At an equilibrium $z=\sqrt{R}\,e^{i\theta}$, the condition that the trace be zero becomes

$$R=\frac{-\cos\alpha}{2\cos\varphi}.$$

Plugging this into (3.2) and taking the absolute value gives

$$1-\frac{\cos^2\varphi}{b^2}=\left(\frac{2\cos\varphi}{b}\tan\alpha-\frac{\sin\varphi}{b}\right)^2,$$

or

$$\tan\alpha=\frac{1}{2\cos\varphi}\left(\sin\varphi\pm\sqrt{b^2-\cos^2\varphi}\right). \tag{3.7}$$

A straightforward calculation, which we will do explicitly in the proof of Lemma 3.6(b), allows us to select the sign and the values of φ that lead to a saddle rather than a node (see Remark 3.7). Since the determinant at a node is positive, we do indeed have a Hopf bifurcation of secondary equilibria for such points. It is shown in [Wang 1990] that the bifurcating limit cycles are repelling. □

Remark 3.2. The surface of trace zero at saddles, that is, the complement of T_+ in the locus of (3.7), is denoted T_-. It intersects the plane $b=1$ in the lines $\alpha=0$ and $\alpha=\varphi-\pi$. It is not part of the bifurcation set, but it is nonetheless relevant to us because its intersection with ⌘ is a codimension-two bifurcation curve, giving rise to a surface ◎ of saddle-nodes of limit cycles (see Section 3.2).

T_- has a fold with respect to α where the radical in (3.7) vanishes, that is, for $b^2=\cos^2\varphi$; this gives

$$\varphi=\pi+\arccos b,\qquad \alpha=\arccos\frac{2b}{\sqrt{3b^2+1}}$$

as the equation of the fold. The projection of this curve in the (b,φ)-plane coincides with the curve ⊙S of Figure 1 (see also Figure 9, top left). As $b\to 1-$, the fold degenerates to the corner $(\varphi,\alpha)=(\pi,0)$, and T_- becomes vertical.

Remark 3.3. For $b=0$ there is a neutral cycle for $\alpha=\varphi-\pi$. For $b=1$ the two surfaces of saddle-node bifurcations have the folds $\alpha=\varphi-\pi\mp\pi/2$. There is a node moving to ∞ for $b\to 1-$, as can be seen from the expression

$$R=\frac{-e^{i\alpha}}{e^{i\varphi}+be^{-4i\theta}};$$

compare (3.1).

Proposition 3.4. *The system is Hamiltonian if and only if $\varphi = 3\pi/2$, $\alpha = \pm\pi/2$, and $b \in \mathbb{R}^+$.*

We call these two line segments in parameter space the *Hamiltonian lines*; Figure 8 shows the generic Hamiltonian phase portraits. The proposition follows immediately from (3.6).

Remark 3.5. The perturbations from the Hamiltonian cases have been studied in [Neishtadt 1978], where it is shown that there is a special value $\gamma \approx 1/4.1100$ with the following property. No limit cycles bifurcate from the point $(b, 3\pi/2, \pi/2)$ if $b < \gamma$, and two limit cycles bifurcate when $b \in (\gamma, 1)$; see phase portrait 8 in Figure 4.

Lemma 3.6. *The local surfaces of Theorem* 3.1 *intersect in the following curves of local codimension-two bifurcations* (compare the first list of curves in Section 2; we use the same notation for the lifted curves as for their projections).

(a) *A curve* $\odot$S, *with equation* $\varphi = \pi + \arccos b$, $\alpha = \pi/2$, *where the second saddle-node bifurcation coincides with the second Hopf bifurcation at the origin.*

(b) *A curve* BT *of Bogdanov–Takens points on the second saddle-node bifurcation*:

$$\varphi = \pi + \arccos\sqrt{\frac{b^2(1-b^2)}{3b^2+1}},$$
$$\alpha = \varphi - \pi - \arcsin b.$$

Proof. (a) This is clear from the formulas in parts (a) and (c) of Theorem 3.1.

(b) A Bogdanov–Takens point requires the trace to be zero at the time of a saddle-node bifurcation. Using the formulas $\alpha = \varphi - \pi \mp \arcsin b$ for S_1 and S_2, we get

$$\cos\alpha = -\sqrt{1-b^2}\cos\varphi \mp b\sin\varphi,$$
$$R = 1/\sqrt{1-b^2},$$

where we have used (3.5) and basic trigonometry. From (3.6), the condition that the trace be zero is then

$$-\sqrt{1-b^2}\cos\varphi \mp b\sin\varphi + 2\frac{\sqrt{1-b^2}}{1-b^2}\cos\varphi = 0,$$

or

$$\tan\varphi = \pm\frac{1+b^2}{b\sqrt{1-b^2}}.$$

Inside the region of interest $\tan\varphi$ is positive, so we must be on S_1. The desired formulas follow readily. □

Remark 3.7. Note that T_- and T_+ meet one another and S_1 along the curve BT. This allows us to differentiate between T_- and T_+ in the locus of (3.7), completing the proof of Theorem 3.1(d). The surfaces T_- and T_+ also meet along the Hamiltonian line $b \in [0, 1]$, $\varphi = 3\pi/2$, $\alpha = \pi/2$.

We show in the top left panel of Figure 9 all the local surfaces of codimension-one bifurcations of Theorem 3.1, plus the surface T_- of trace zero at the saddles (Remark 3.2). To help interpret this figure, Figure 11 shows cross sections of the same surfaces for various values of b. Note that the line segment $b = 1$, $\varphi = 3\pi/2$, $\alpha \in [0, \pi/2]$ is part of T_+, the surface of Hopf bifurcations of secondary equilibria.

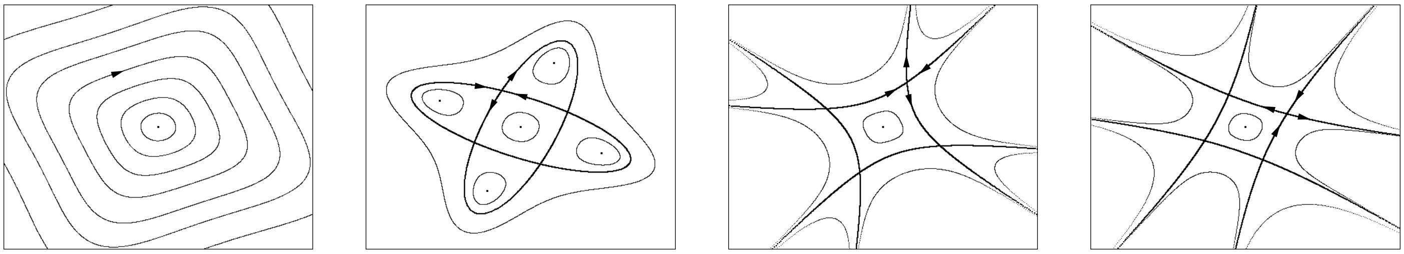

FIGURE 8. Generic phase portraits along the Hamiltonian lines (see Proposition 3.4). Left: $\alpha = -\pi/2$ and $0 < b < 1$. Center left: $\alpha = \pi/2$ and $0 < b < 1$. Center right: $\alpha = -\pi/2$ and $b > 1$. Right: $\alpha = \pi/2$ and $b > 1$.

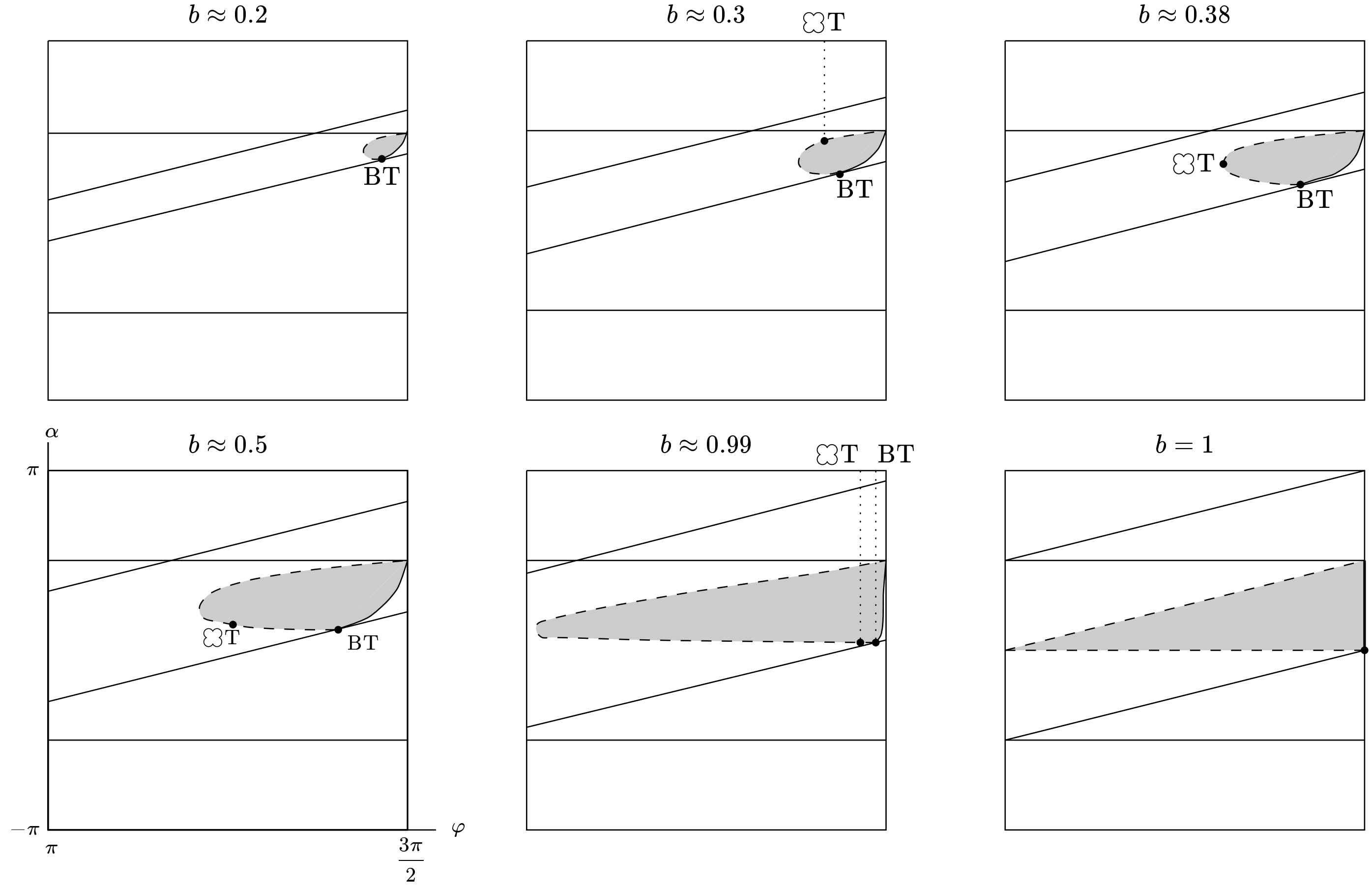

FIGURE 11. Sketches of cross sections of Figure 9 (top left) for various values of b. The horizontal lines are the cross sections of the Hopf bifurcation surfaces $\odot$. The diagonal lines come from S_1 and S_2. The solid arc comes from T_+, where the secondary equilibria undergo a Hopf bifurcation, and the dashed arc comes from T_-, which is not in the bifurcation set. The region bounded by the two arcs is shaded for clarity. The features mentioned in Remark 3.2 are visible here. Note the presence, for $b > \gamma \approx 1/4.11$, of the point ⌘T for which there is a clover connection with trace zero. As b increases further, this point crosses over the fold of T_-.

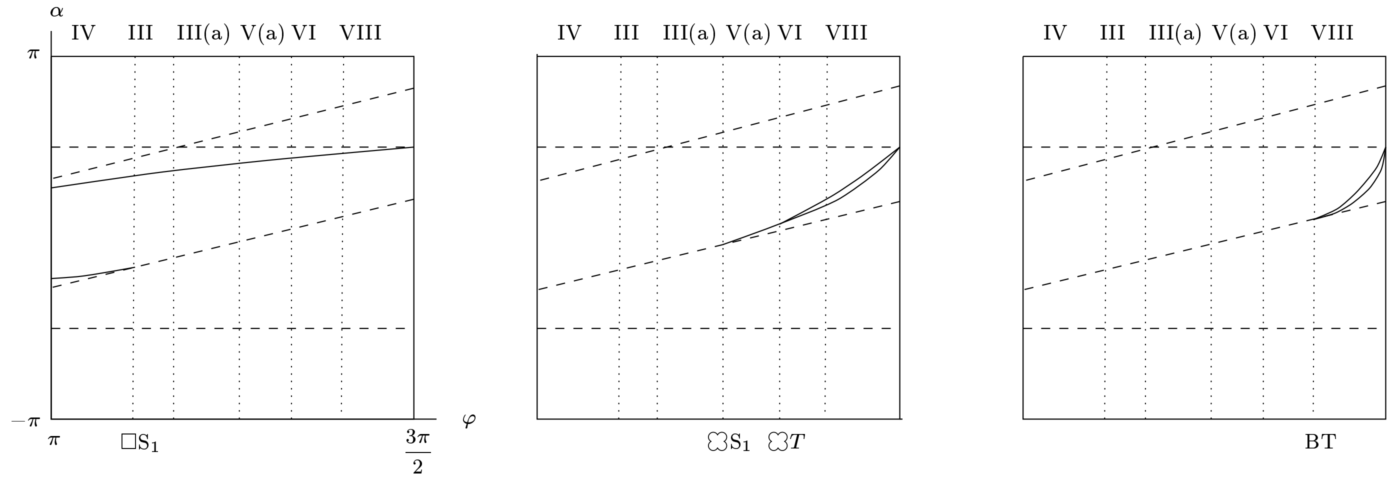

FIGURE 12. Sketches of cross sections of the last three panels in Figure 9, for $b \approx 0.8$. The dashed curves come from $\odot$, S_1 and S_2. The solid lines come from $\Box$ (left), from ⌘ and $\circledcirc$ (middle), and from T_+ and ♀ (right).

3.2. The Nonlocal Surfaces for $b \in [0, 1]$

This section presents the model of the bifurcation set in the cube of interest. The dashed boundary curves in the (b, φ)-plane lift to nonlocal curves in (b, φ, α)-space, and the lifts lie on local surfaces. This is no contradiction. The fact that we do not have a parametrization for a nonlocal curve means that its exact position on the local surface is known by numerical methods only.

Proposition 3.8. (a) *The curve* $\Box\mathrm{S}_1$ *lifts to a curve on* S_1; *the lift is the intersection of* S_1 *with a surface* $\Box$ *of square connections.*
(b) *The curve* $\Box\mathrm{S}_2$ *lifts to* S_2; *the lift is the intersection of* S_2 *with* $\Box$.
(c) *The curve* ✤S_1 *lifts to* S_1; *the lift is the intersection of* S_1 *with a surface* ✤ *of clover connections.*
(d) *The curve* ✤T *lifts to the surface* T_- *where the trace is zero at the saddles*; *the lift is the intersection of* T_- *with* ✤, *and crosses the fold of* T_-.

This follows from the definitions. As with the local curves, we denote the lifts in (b, φ, α)-space by the same symbols as the projections in the (b, φ)-plane.

Remark 3.9. The curves $\Box\mathrm{S}_1$ and $\Box\mathrm{S}_2$ extend to the adjoining cube $\varphi \in [\pi/2, \pi]$, and are exchanged by the symmetry $(\varphi, \alpha) \mapsto (-\varphi, -\alpha)$: see Figure 13.

The curves of Proposition 3.8 are shown in Figure 9 (top left) on the saddle-node surfaces and the trace-zero surface. See also Figure 11.

We know what codimension-one bifurcations occur in what regions from the inventory of the bifurcation sequences [Krauskopf 1994]. Furthermore, we have some information on the boundaries of the surfaces because of the knowledge of the nonlocal curves. This allows us to *model* the remaining surfaces, by which we mean to determine topologically where they lie in the bifurcation set, even though we cannot explicitly write their values of α as a function of b and φ. The modeled surfaces will then describe the topology of the bifurcation set even though their exact shapes are unknown. It is also possible to calculate cross sections of the nonlocal surfaces by continuation, to determine their shape.

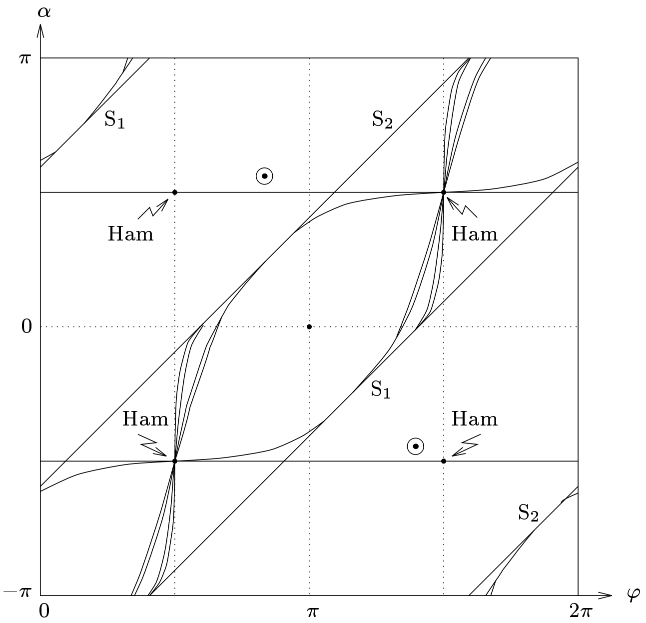

FIGURE 13. A sketch of the torus (φ, α) for $b \approx 0.8$, showing how the picture for all φ can be constructed from the portion $\varphi \in [\pi, 3\pi/2]$ by 180° rotations around the points $(\pi, 0)$ and $(3\pi/2, \pi/2)$. The figure also shows how the surfaces of square connections are mapped to each other; see also Figure 14.

For the modeling we need the following assumption:

Assumption 3.10. *There are no intersections of nonlocal surfaces with other surfaces apart from the known curves of codimension-two bifurcations. In addition, the nonlocal surfaces do not have folds with respect to* α.

Remark 3.11. The validity of this assumption is part of the conjecture that (1.2) is a versal unfolding in the open regions of the (b, φ)-plane. It has been checked numerically by calculating cross sections of the nonlocal surfaces with the program Auto. See Section 4 for more details.

A nonlocal surface of codimension-one bifurcations is determined by its boundary. In the boundary we have typically a certain nonlocal curve of bifurcations of codimension two, and a segment of a Hamiltonian line. We may, however, be lacking some knowledge of how exactly the surface intersects the boundary of the cube. Then we are left with a piece of the boundary of the surface that is not closed. Under Assumption 3.10 we can model the surface if we know its shadow in the (b, φ)-plane. This question can be settled by showing that the codimension-one bifurcation in question is in the bifurcation sequence for some (b, φ) in a given region. This can be checked by perturbation methods around the boundary, or simply by investigating bifurcation sequences by computer. We refer to [Krauskopf 1994] for an inventory of all bifurcation sequences.

Under Assumption 3.10 we can prove this result:

Theorem 3.12. *The following nonlocal surfaces are in the bifurcation set* (see Figure 9, top right and bottom, and Figure 12).

(a) *Two surfaces of square connections, denoted* $\square$. *The upper surface extends from the curve* $\square\mathrm{S}_2$ *on* S_2 *to the Hamiltonian line* $\varphi = 3\pi/2$, $\alpha = \pi/2$, $b \in [0,1]$. *The lower surface extends from the curve* $\square\mathrm{S}_1$ *on* S_1 *to the line* $\varphi = \pi/2$, $\alpha = -\pi/2$. (The two surfaces are exchanged by the symmetry $(\varphi, \alpha) \mapsto (-\varphi, -\alpha)$ when extended to the adjoining cube: see Remark 3.9 and Figure 13.)
(b) *The surface of clover connections, denoted* ⌘. *It extends from the curve* ⌘S_1 *on* S_1 *to the line* $\varphi = 3\pi/2$, $\varphi = \pi/2$, $b \in [0,1]$.
(c) *The surface of saddle-node bifurcations of limit cycles, denoted* $\circledcirc$. *It lies above the surface of clover connections, and extends from the curve* ⌘T *on* T_- *to the Hamiltonian line* $\varphi = 3\pi/2$, $\alpha = \pi/2$, $b \in [\gamma, 1]$.
(d) *The surface of homoclinic connections of secondary equilibria, denoted* ♀. *It lies above the surface* T_+ *of Hopf bifurcations of secondary equilibria, emerging from the curve* BT *on* S_1 *and extending to the line* $\varphi = 3\pi/2$, $\alpha = \pi/2$, $b \in [0,1]$.

Proof. (a) The curve $\square\mathrm{S}_2$ and the Hamiltonian line $\varphi = 3\pi/2$, $\alpha = \pi/2$, $b \in [0,1]$ are in the boundary of the upper surface. Square connections can be found in all regions except II. The curve $\square\mathrm{S}_1$ and the Hamiltonian line $\varphi = 3\pi/2$, $\alpha = -\pi/2$, $b \in [0,1]$, where the phase portrait is equivalent to the one in Figure 8 (center left) with the arrows reversed, are in the boundary of the lower surface. Square connections, with the reversed direction of arrows, can only be found in region IV. We remark that both surfaces extend into region I ($b > 1$), as will be discussed in Section 3.3.

(b) The curve ⌘S_1 and the Hamiltonian line $\varphi = 3\pi/2$, $\alpha = \pi/2$, $b \in [0,1]$ are in the boundary of this surface. Clover connections can be found in regions V, VI, VII and VIII.

(c) The curve ⌘T and the Hamiltonian line $\varphi = 3\pi/2$, $\alpha = \pi/2$, $b \in [\gamma, 1]$ are in the boundary of this surface. The point of intersection γ of ⌘T with the Hamiltonian line has been calculated in [Neishtadt 1978]. The existence of the surface follows from the perturbation results there. It is also possible, but difficult, to find the two limit cycles numerically in regions VI and VIII [Krauskopf 1994; Malo 1994]; see Figure 4, panel 8.

(d) The curve BT and the Hamiltonian line $\varphi = 3\pi/2$, $\alpha = \pi/2$, $b \in [0,1]$ are in the boundary of this surface. Homoclinic connections of the secondary equilibria can be found in regions VII and VIII, as is to be expected close to the line BT. $\square$

Remark 3.13. By the nature of the boundary curves, the line segment $b = 1$, $\varphi = 3\pi/2$, $\alpha \in [0, \pi/2]$ is part of the surfaces ⌘, $\circledcirc$ and ♀. It is also part of T_+, as can be seen from the formula in Theorem 3.1(d).

Theorem 3.12 is illustrated in Figure 9. The top right panel shows the upper and lower surfaces $\square$ of square connections. The bottom left panel shows the surface ⌘ of clover connections, and above it the surface $\circledcirc$ of saddle-nodes of limit cycles. The bottom right panel shows the surface ♀ of homoclinic connections of secondary equilibria, above

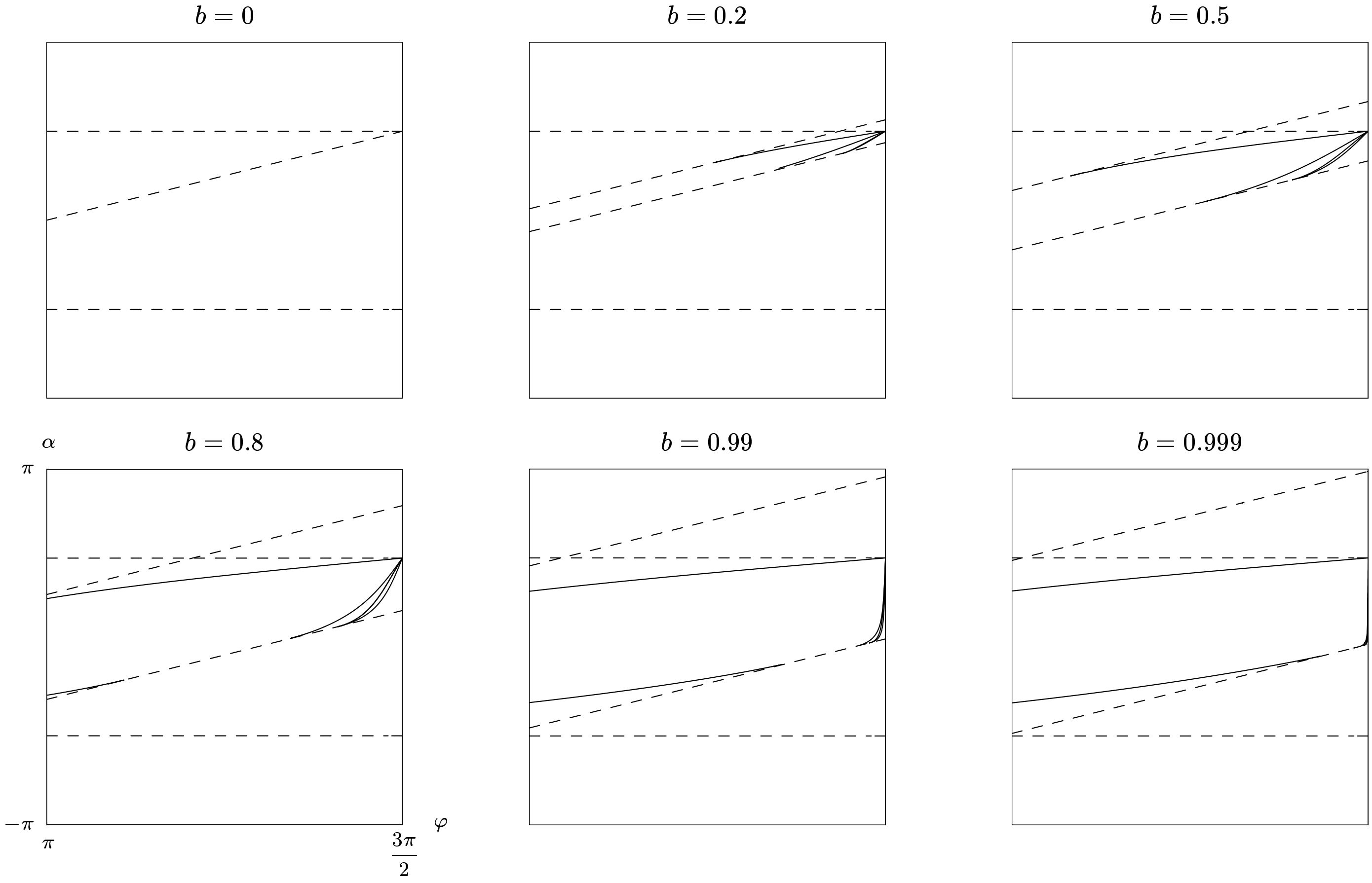

FIGURE 14. Cross sections of the bifurcation set of Figure 10 for various $b < 1$, calculated with Auto. The dashed lines are as in Figure 12, the solid lines at $b = 0.8$ connecting to the point $\varphi = 3\pi/2$, $\alpha = \pi/2$ are, from the bottom up: T_+, ♀, ✤, □ (◎ could not be calculated). Note how T_-, ♀ and ✤ (and ◎) accumulate on the line segment $b = 1$, $\varphi = 3\pi/2$, $\alpha \in [0, \pi/2]$.

the surface T_+ of Hopf bifurcations of secondary equilibria. The shadow of each surface is shown at the top or bottom.

To give a better idea of the nonlocal surfaces, Figure 10 shows perspectives of the whole model in the cube of interest with the surfaces partially cut open, and Figure 12 shows sketches of their cross sections for $b \approx 0.8$.

While Figure 12 is a qualitative sketch, Figure 14 shows actual cross sections, for various $b < 1$, calculated with Auto. The cross sections show all surfaces except for the surface ◎ of saddle-node bifurcations of limit cycles, which is very difficult to continue numerically due to the proximity of the cycles to the saddle points. In any case ◎ would be indistinguishable from ✤ in this figure: for example, for $b = 0.8$ and $\varphi = 4.6$ the clover connection occurs at $\alpha \approx .99957$, while the bifurcation of saddle-node limit cycles occurs at $\alpha \approx 1.00145$.

There are eleven regions of generic phase portraits in the cube of interest. They were shown in Figure 4 grouped around a sketch of the cross section of the bifurcation set for $b \approx 0.8$. We remark that the surfaces of codimension-one bifurcations are divided into different parts by the curves of codimension-two bifurcations on them. For example, the saddle-node bifurcation one gets by moving from region 2 to region 3 has a different global structure from the saddle-node bifurcation one gets by moving from region 2 to region 4. We do not

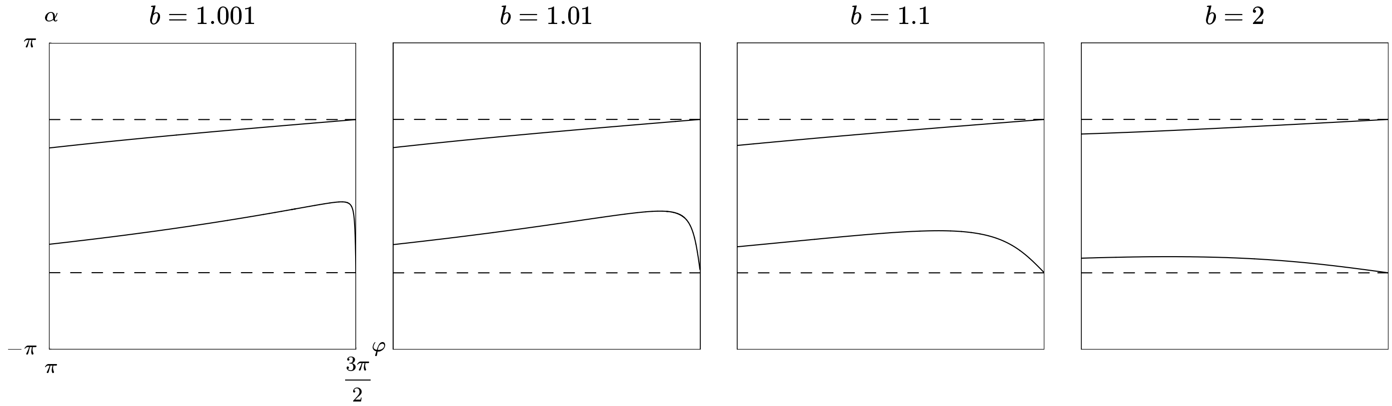

FIGURE 15. Cross sections of the bifurcation set for various values of $b > 1$, calculated with Auto. The dashed lines are the surfaces of Hopf bifurcations, the solid lines are the surfaces of square connections. The latter do not intersect other surfaces other than in the known curves, and appear to be without folds with respect to α. The lower surface accumulates on the line segment $b = 1$, $\varphi = 3\pi/2$, $\alpha \in [-\pi/2, 0]$.

give pictures of the different cases of codimension-one bifurcations since they can be constructed from the generic phase portraits of Figure 4. They can also be found as parts of the bifurcation sequences in [Krauskopf 1994].

3.3. The Bifurcation Set for $b > 1$

We now discuss the bifurcation set for region I, that is, $b > 1$. As mentioned earlier, there are four secondary equilibria for any value of α, and they are saddles. The surfaces that extend out of the cube into region I are $\odot$ and $\square$:

Theorem 3.14. *For $b > 1$ the following surfaces of codimension-one bifurcations are in the bifurcation set.*

(a) *Two planes $\odot$ of Hopf bifurcations of the origin, with equation $\alpha = \pm\pi/2$. The limit cycles occur for $-\pi/2 < \alpha < \pi/2$ and are attracting.*
(b) *Two surfaces $\square$ of square connections. The upper surface extends from the line $\varphi = \pi/2$, $\alpha = \pi/2$ to the line $\varphi = 3\pi/2$, $\alpha = \pi/2$. The lower surface extends from the line $\varphi = \pi/2$, $\alpha = -\pi/2$ to the line $\varphi = 3\pi/2$, $\alpha = -\pi/2$.* (The two surfaces are exchanged by the symmetry $(\varphi, \alpha) \mapsto (-\varphi, -\alpha)$ when extended to the adjoining cube: see Remark 3.9 and Figure 13.)

Proof. (a) See the proof of Theorem 3.1 (a).

(b) The boundary lines of the surfaces are the lines where the system is Hamiltonian, as shown in Figure 8 (center right and far right). The two square connections can both be found in region I. $\square$

The situation is depicted in Figure 15 by a series of cross sections calculated with Auto for different values of $b > 1$. Since Figure 15 makes it quite clear what happens in this simple case, we have not included a three-dimensional picture. The four generic phase portraits for $b > 1$ were shown in Figure 5, together with a typical cross section.

Remark 3.15. For $b = 1$ the lower surface of square connections contains the line segment $b = 1$, $\varphi = 3\pi/2$, $\alpha \in [-\pi/2, 0]$, since $\square S_1$ lies on S_1; see Figure 15 (left).

4. ON THE GENERICITY OF THE BIFURCATIONS

The compact equation (1.2) is conjectured to be a versal unfolding in the open regions of the (b, φ)-plane. Furthermore, it is conjectured that there are no bifurcation sequences other than the known ones. One possibility to deal with these conjectures is to prove statements on the number of limit cycles that can occur in a particular region of the (b, φ)-plane. This allows conclusions about the bifurcation sequence that can occur in the region. For results of this kind we refer to [Cheng 1990; Cheng and Sun 1992; Wan 1978; Zegeling 1993]. We take a geometrical approach and try to extract as much information as possible from the knowledge of the bifurcation set about the question of versality. This allows tentative conclusions supported by numerical evidence, and indicates directions for further research and towards rigorous proofs.

The first issue is whether the codimension-one bifurcations are generic. We have modeled the nonlocal surfaces under Assumption 3.10 that they intersect other surfaces only in the known curves of codimension-two bifurcations and do not have folds with respect to α. Even though we cannot prove Assumption 3.10, there is strong numerical evidence for it. The first indication for its validity is the fact that no unknown bifurcation sequences have been found, either by theoretical work or by numerical studies. The author has done a thorough study of the bifurcation sequences in [Krauskopf 1994] with the program DsTool. However, it is not possible to study the whole parameter space in this fashion, so there is the possibility that phenomena have been overlooked that are very small in parameter space or phase space. See the discussion in [Krauskopf 1994; Malo 1994] about finding the two limit cycles in regions VI and VIII.

The strongest support for Assumption 3.10 is from the calculation of cross sections of the bifurcation set by continuation with Auto. We briefly indicate how the continuation has been carried out. It is straightforward to calculate and continue local bifurcations. The homoclinic connections of secondary equilibria have been approximated by limit cycles of very high period in the continuation. A boundary value approach has been used to calculate and continue the square and clover connections. We have not succeeded yet in continuing the saddle-nodes of limit cycles. Since the limit cycles are extremely close to the saddle points in this case, there are problems with the convergence of the continuation algorithms.

The cross sections not only provide evidence for Assumption 3.10, but also give a clear picture of the actual shape of the surfaces, as seen in Figures 14 and 15. In principle it is possible to calculate the entire bifurcation set by continuation techniques, for example by calculating a sufficient number of cross sections. Further work on continuation, including the calculation of the surface of saddle-nodes of limit cycles and the nonlocal curves of bifurcations of codimension two, is in progress.

It is possible that there are yet unknown curves of codimension-two bifurcations on the surfaces of codimension-one bifurcations. However, we have not found any evidence for that in the experiments. Unless such a curve is a closed loop, which seems unlikely, it will have to intersect another curve of codimension-two bifurcations, and thus should be detectable by continuation.

This leads to the next issue, the discussion of the curves of codimension-two bifurcations. Are there points of higher codimension on them from which yet unknown surfaces of codimension-one bifurcations emerge?

First we show that the known curves of bifurcations of codimension two in (b, φ, α)-space do not intersect for $\varphi \neq 3\pi/2$. This is not apparent if one only looks at the (b, φ)-plane, as in Figure 1. Four questions arise: Does BT intersect ✤T? Does $\odot$S intersect ✤S_1 and $\square\mathrm{S}_2$? Do $\square\mathrm{S}_1$ and $\square\mathrm{S}_2$ meet for $\varphi = \pi$? Is there a tangency of ✤T with $\odot$S?

It follows easily by considering the respective curves in (b, φ, α)-space that the answer to the first two questions is no. Next, $\square\mathrm{S}_1$ and $\square\mathrm{S}_2$ lie respectively on S_1 and S_2, and are interchanged by the symmetry $(\varphi, \alpha) \to (-\varphi, -\alpha)$. Therefore they do not intersect in (b, φ, α)-space, but their projections meet for $\varphi = \pi$; compare Figure 9 (top left).

We now address the fourth question. Note that it is not clear by just looking at the (b, φ)-plane if there really is a tangency of the curve ✤T, since this curve is known by continuation only. However, considering the bifurcation set we conclude this:

Lemma 4.1. *There is a tangency of the curve* ✤T *with* $\odot$S *in the* (b, φ)*-plane. The respective curves of codimension-two bifurcations in* (b, φ, α)*-space do not have a tangency.*

Proof. Even though the nonlocal curve ꕤT is known by continuation only, it lifts to a curve on T_-, which is known to start at $(b, \varphi, \alpha) = (1,\, 3\pi/2,\, 0)$ and end at $(\gamma,\, 3\pi/2,\, \pi/2)$; see Proposition 3.8(d). It follows that the lift has to go over the fold of T_-, even if we do not know exactly where, a remark due to A. I. Khibnik. Since this fold has the same projection $\varphi = \arccos b$ as the intersection $\odot$S of the second Hopf and saddle-node surfaces, we have shown that there is indeed a tangency in the (b, φ)-plane. However, for the fold curve we have

$$\alpha = \arccos \frac{2b}{\sqrt{3b^2+1}} < \pi/2$$

for $b \in (0, 1)$; see Lemma 3.6(b). Consequently, ꕤT lies well below the plane $\alpha = \pi/2$ of Hopf bifurcations and there cannot be a tangency in (b, φ, α)-space. $\square$

The argument of the proof becomes very clear in Figure 9, where ꕤT can be seen going over the fold of T_-. See also the cross sections in Figure 11.

Corollary 4.2. *There is no difference between the bifurcation sequences in regions* V(a) *and* V(b)*. Hence there are eleven bifurcation sequences, as opposed to the twelve regions into which the* (b, φ)*-plane is divided.*

The next question is whether the codimension-two bifurcations are generic—that is, whether a transversal section of such a curve shows locally, around the point of intersection, the two-dimensional bifurcation diagram expected for the generic codimension two bifurcation in question. There are three cases:

(a) Bogdanov–Takens points on BT;
(b) saddle-node separatrix loops on $\square\mathrm{S}_1$, $\square\mathrm{S}_2$ and ꕤS_1; and
(c) separatrix loops with trace zero on ꕤT.

Transversal sections to the curves do indeed show the bifurcation diagrams expected for the respective generic cases. See Figure 12 and compare the right panel with [Bogdanov 1976; Takens 1974], the left and middle panels with [Schecter 1987], and the middle panel with [Chow et al. 1990; Nozdracheva 1982]. Note that in the last two cases it is necessary to divide out the $\mathbb{Z}_4$-symmetry to reduce the heteroclinic connections to separatrix loops in order to apply the results from the literature. A complete proof would consist of showing that certain normal form coefficients are nonzero along the curves of codimension-two bifurcations. This is beyond the scope of this paper. We summarize the discussion as follows:

Claim. *For* $\varphi \neq 3\pi/2$ *the known bifurcations of codimension one and two of* (1.2) *unfold generically in the given parameters* b, φ *and* α. *There are no points of codimension higher than two on the curves of codimension-two bifurcations.*

The last issue we address concerns the bifurcations at the boundary of the cube of interest ($\varphi = 3\pi/2$), which can give rise to surfaces of codimension-one bifurcations for $\varphi \neq 3\pi/2$. The classic example for this phenomenon is the study of the Hamiltonian cases for $\alpha = \pm\pi/2$ [Neishtadt 1978]. The knowledge of what can bifurcate from the different Hamiltonian cases played an important role in finding the list of known bifurcation sequences. The Hamiltonian cases organize the codimension-one bifurcation surfaces. This can be seen in the three-dimensional view in Figure 10 and in the cross sections in Figures 13 and 14.

An open problem is the role played by the bifurcations for $(b, \varphi) = (1,\, 3\pi/2)$, corresponding to $A = -i$ in the model equation (2.1). With the knowledge of the bifurcation set we can say the following. The surfaces $\odot$ of Hopf bifurcations and ᕋ of homoclinic loops of the secondary equilibria, the surface ꕤ of clover connections and the surface $\circledcirc$ of saddle-nodes of limit cycles accumulate on the line segment $b = 1$, $\varphi = 3\pi/2$, $\alpha \in [0,\, \pi/2]$. This is visible in Figures 10 and Figure 14. Due to symmetry the same types of surfaces accumulate on the line segment $b = 1$, $\varphi = 3\pi/2$, $\alpha \in [\pi/2, \pi]$; compare Figure 13. The lower surface of square connections accumulates on the line segment $b = 1$,

$\varphi = 3\pi/2$, $\alpha \in [-\pi/2, 0]$, as shown in Figure 15. Again due to symmetry the same type of surface accumulates on the line segment $b = 1$, $\varphi = 3\pi/2$, $\alpha \in [-\pi, -\pi/2]$.

This means that the line $b = 1$, $\varphi = 3\pi/2$, $\alpha \in (-\pi, \pi]$ is of codimension at least two, with points of higher codimension at $\alpha = -\pi/2,\ 0,\ \pi/2,\ \pi$. The study of these bifurcations turns out to be the study of the bifurcations at infinity of (1.2). They organize the bifurcation set in much the same way as the Hamiltonian cases. Further work on the bifurcations at infinity is in progress and will be the topic of a later publication.

ACKNOWLEDGMENTS

It is a pleasure to thank H. W. Broer, E. Doedel, J. Guckenheimer, P. Holmes, A. I. Khibnik, M. Krupa, Yu. A. Kuznetsov, C. Rousseau and F. Takens for fruitful discussions, encouragement and help.

I also thank S. Levy for his excellent cooperation during editing, and for his valuable remarks and suggestions.

The support of the Centre de Recherches Mathématiques, Montréal, Canada is gratefully acknowledged.

REFERENCES

[Arnol'd 1977] V. I. Arnol'd, "Loss of stability of self-oscillation close to resonance and versal deformations of equivariant vector fields", *Functional Anal. Appl.* **11** (1977), 85–92.

[Arnol'd 1988] V. I. Arnol'd, *Geometrical Methods in the Theory of Ordinary Differential Equations*, 2nd ed., Springer, New York, 1988.

[Arnol'd et al. 1994] V. I. Arnol'd et al., *Dynamical Systems V: Bifurcation Theory and Catastrophe Theory*, Encyclopedia of Mathematical Sciences **5**, Springer, Berlin, 1994.

[Back et al. 1992] A. Back et al., "DsTool: Computer assisted exploration of dynamical systems", *Notices Amer. Math. Soc.* **39** (1992), 303–309.

[Berezovskaia and Khibnik 1978] F. S. Berezovskaia and A. I. Khibnik, "On the analysis of the equation $\dot{z} = e^{i\alpha}z + Az\,|z|^2 + \bar{z}^3$ (in connection with the problem of stability loss of a periodic solution near 1:4 resonance)", Report, Research Computing Center Acad. Sci. USSR, Pushchino, 1978 (in Russian).

[Berezovskaia and Khibnik 1979] F. S. Berezovskaia and A. I. Khibnik, "On the problem of auto-oscillation bifurcations near 1:4 resonance (investigation of the model equation)", preprint, Research Computing Center Acad. Sci. USSR, Pushchino, 1979 (in Russian).

[Berezovskaia and Khibnik 1980] F. S. Berezovskaia and A. I. Khibnik, "On the bifurcations of separatrices in the problem of stability loss of auto-oscillations near 1:4 resonance", *Prikl. Math. Mech.* **44** (1980), 663–667.

[Bogdanov 1976] R. I. Bogdanov, "Versal deformation of a singularity of a vector field on the plane in case of zero eigenvalues", *Sel. Math. Sov.* **1** (1981), 389–421.

[Carr 1981] J. Carr, *Applications of Centre Manifold Theory*, Applied Mathematical Science **35**, Springer, New York, 1981.

[Cheng 1990] C.-Q. Cheng, "Hopf bifurcations in nonautonomous systems at points of resonance", *Science in China* A**33** (1990), 206–219.

[Cheng and Sun 1992] C.-Q. Cheng and Y.-S. Sun, "Metamorphoses of phase portraits of vector fields in the case of symmetry of order 4", *J. Diff. Eq.* **95** (1992), 130–139.

[Chow 1994] S.-N. Chow, C. Li and D. Wang, *Normal Forms and Bifurcation of Planar Vector Fields*, Cambridge University Press, Cambridge, 1994.

[Chow et al. 1990] S.-N. Chow, B. Deng and B. Fiedler, "Homoclinic bifurcations at resonant eigenvalues", *J. Dyn. Diff. Eq.* **2** (1990), 177–244.

[Doedel 1986] E. Doedel, "Auto: Software for continuation and bifurcation problems in ordinary differential equations", California Institute of Technology, Pasadena, California, 1986.

[Krauskopf 1994] B. Krauskopf, "Bifurcation sequences at 1:4 resonance: an inventory", *Nonlinearity* **7** (1994), 1073–1091.

[Malo 1994] S. Malo, "Rigorous computer verification of planar vector field structure", Ph.D. Thesis, Cornell University, Ithaca, 1994.

[Neishtadt 1978] A. I. Neishtadt, "Bifurcations of the phase patterns of an equation system arising in the problem of stability loss of selfoscillation close to 1:4 resonance", *Prikl. Math. Mech.* **42** (1978), 896–907.

[Nozdracheva 1982] V. P. Nozdracheva, "Bifurcation of a noncoarse separatrix loop", *Diff. Eq.* **18** (1982), 1098–1104.

[Schecter 1987] S. Schecter, "The saddle-node separatrix loop bifurcation", *SIAM J. Math. Anal.* **18** (1987) 1142–1156.

[Takens 1974] F. Takens, "Forced oscillations and bifurcations", in *Applications of Global Analysis I*, Communications of the Mathematical Institute **3**-1974, Rijksuniversiteit Utrecht, 1974.

[Wan 1978] Y.–H. Wan, "Bifurcation into invariant tori at points of resonance", *Arch. Rat. Mech. Anal.* **68** (1978), 343–357.

[Wang 1990] D. Wang, "Hopf bifurcation at the nonzero foci in 1:4 resonance", *Acta Math. Sinica* (new series) **6** (1990), 10–17.

[Zegeling 1993] A. Zegeling, "Equivariant unfoldings in the case of symmetry of order 4", *Serdica* **19** (1993), 71–79.

Bernd Krauskopf, Vakgroep Wiskunde, Rijks*universiteit* Groningen, Postbus 800, 9700 AV Groningen, Nederland (bernd@math.rug.nl)

Received April 1, 1994; accepted in revised form August 29, 1994